Modular architecture of a Multi-frequency Electrical Impedance Tomography system: design and implementation

Alexandre Fouchard, Alain Noca, Stéphane Bonnet, Pascale Pham,
Valérie Sinniger, Didier Clarençon and Olivier David

***Abstract*— Electrical impedance tomography (EIT) provides means of imaging the electrical properties distribution of biological tissues and fluids while impedance spectroscopy (IS) allows measuring their frequency response in a more global way. Both require precise and well-integrated instrumentation. In this work, we propose a modular architecture of a multi-frequency EIT (MfEIT) system which has capabilities in implementing both IS and MfEIT. First, IS performance is assessed *in vivo* using a cuff electrode implanted around the rodent cervical vagus nerve. Second, MfEIT performance is evaluated *in vitro* based on saline phantom experiments. Overall system allows addressing a wide range of applications and proves effective both *in vitro* and *in vivo*.**

I. Introduction

Medical Electrical Impedance Tomography (EIT) [1], [2] and Impedance Spectroscopy (IS) [3] are two complementary electrical characterization techniques of biological tissues and fluids. Both rely on impedance measurements to extract respectively internal electrical properties, e.g. conductivity and permittivity at the mesoscopic scale, or the impedance spectrum of the studied medium. Since electrical properties are material specific [4] and show dependences on physiological and pathological functions, EIT and IS provide unique ways to infer the internal structure of the objects under study and to monitor their activity. Using low frequency low level alternating electrical fields, both techniques prove to be non-ionizing and offer capabilities of continuous monitoring. They can be implemented using portable and low cost instrumentation, compared to other imaging modalities such as MRI or CT-scan [2].

Transduction in IS and EIT is ensured through electrodes whether affixed on the surface of the medium under study or positioned within the medium. *In vivo* measurements are conducted using the two-electrode or four-electrode method [1] It allows to sense both the medium and the interfacial effects for their electrical properties. IS and EIT usually use a network of electrodes specifically designed in order to maximize the sensitivity of the measurements for a given application. Patterns of electric fields are injected in the object through drive electrodes and the response of the object is measured using either the same electrodes (two-electrode configuration) or other pairs of electrodes (four-electrode method).

Requirements in terms of instrumentation are quite demanding. A wide range of trans-impedances has to be addressed, combined with a bandwidth ranging from a few hertz up to 10MHz. Furthermore, both ranges are highly dependent on intended application. For instance, assuming an injected current of $1mA_{rms}$, induced voltages are in the range of a few microvolts to tens of millivolts [1]. Addressing multi-frequency impedance measurements leads to multiple sources of errors in instrumentation [5] that have to be taken into account in the design of an experimental device.

In this paper, we describe a modular architecture for a combined IS and Multi-frequency EIT system. It is designed as a serial single voltage source system in which electrodes are addressed sequentially. The profit comes from the concepts used to measure signal amplitudes and to switch between different electrodes that enable a reduced-consumption operation. While the system specifications allow addressing a wide range of applications in the two application modes, IS performance has currently been assessed *in vivo* on the rodent cervical vagus nerve and EIT operation has been evaluated *in vitro* using data acquired from saline phantom experiments.

II. Methods

A. System overview

Overall system embodies two application modes. In IS, frequency is swept in the desired range to draw an impedance spectrum. In EIT, a constant frequency signal is used, and electrodes are sequentially addressed. The system encompasses three sub-systems organized hierarchically (Fig. 1).

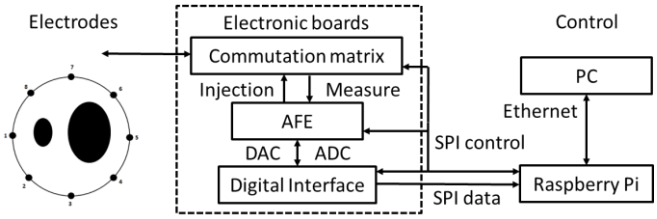

Figure 1. Overview of sub-system interactions

A. Fouchard, A. Noca, S. Bonnet and P. Pham are with the CEA, Leti, MINATEC Campus, Grenoble, France (e-mail: alexandre.fouchard@centraliens-lyon.net, stephane.bonnet@cea.fr).

V. Sinniger, D. Clarençon and O. David are with the Université Joseph Fourier, Grenoble Institute of Neurosciences, Grenoble, France (e-mail: olivier.david@inserm.fr).

D. Clarençon is also with the Institut de Recherche Biomédicale des Armées, Grenoble, France.

978-1-4244-7929-0/14/$26.00 ©2014 IEEE

It includes a general purpose computer acting as a controller, a Raspberry Pi [6] used as a control module and several electronic boards involving discrete components. The electronic boards implement an analog front-end (AFE) for electrical impedance measurements, a commutation matrix and digital interfaces for control and data transmission purposes. Communication between different subsystems is ensured through serial peripheral interface (SPI) and Ethernet links. The system is single-supplied and can be battery powered to provide a floating system.

The profit in using such architecture comes from its pluggable nature: every component may be upgraded and incorporated seamlessly. Software design also benefits from the use of the Raspberry Pi as control module: it is quite straightforward and allows quick prototyping. All code is written in Bash and C allowing an almost real time operation. The library BCM2835 [7] is used to provide high-level C functions to interact with GPIO.

B. *Operating principle*

The system is based on the operating principle of a single voltage source, serial system. It allows electrical measurements using the two-electrode or the four-electrode method. Electrodes are addressed sequentially to inject current and measure induced voltages (Fig. 2). The system encompasses four analog signal buses: two for injection and two for measurements. Each electrode is connected to every bus using four reed relays per electrode. Applied voltage is adjusted in order to get either constant measured voltage or constant measured current. Voltage u and current i measurements are conducted. Their amplitude is determined automatically, and allows impedance norm to be deduced: $\mathrm{norm}(Z) = \mathrm{amp}\, v / \mathrm{amp}\, i$, while their relative phase is currently deduced from oscilloscope readings.

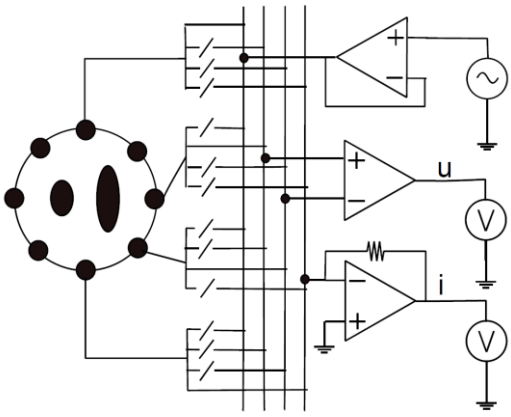

Figure 2. Operating principle of IS and EIT system

In this work, the EIT reconstruction process only involves amplitude values of measured voltages when rotating injection and measurements. Without further refinements, this method lacks information about the sign of measured values. Incorporating a priori sign information in the pre-processing stage of EIT is one the proposals of this work. Signs of each measurement can be predicted by modeling the experimental setup: geometry of the medium to be imaged, consequent electrode positions and data collection strategy.

C. *Electrical impedance measurements*

Electrical impedance measurements involve both digital interface and analog front-end.

The digital interface allows generating a sinusoidal voltage signal through the use of a direct digital synthesizer (DDS), circuit AD9837 from Analog Devices [8]. The output impedance of the generator is then lowered by the use of a voltage buffer, LMV651 from Texas Instruments (TI) [9]. Sinusoidal voltage signal can be generated in this way from 0.1Hz up to 1MHz, by steps of 0.06Hz, and its amplitude may be modulated by external resistor network up to $600\mathrm{mV}_{\mathrm{pp}}$.

Measurement of injected current is done by a trans-impedance amplifier, TI OPA380 [10, p. 380]. Different feedback resistors are included to allow translating a wide range of input currents from 1nA to 10mA. Small currents from 1nA to 1µA can only be converted in the range 0.1Hz to 1kHz due to the limited amplifier gain-bandwidth product.

The instrument amplifier to measure induced voltages is currently worked out with the low noise voltage preamplifier SR560 from Stanford Research Systems [11]. A gain of 100 or 1000 is used in conjunction with a band-pass filter centered on signal frequency.

D. *Signal acquisition*

In this work, signal amplitude of both injected currents and induced voltages are determined by a combination of under-sampling and use of histogram. Signals used in the system are of sinusoidal pattern and exhibit a peculiar form when a histogram of sampling conversion code is plotted (Fig. 3). This allows an easy determination of the signal amplitude. Under-sampling is used to sample the signal and address high frequencies of the spectrum. It involves the Analog to Digital Converter (ADC) ADS7947 from TI, chosen for its analog bandwidth, sufficiently wide to pass excitation frequency, up to 15MHz at 3dB. In the system, pseudo-random sampling is done at 33 kHz, to address the range 100 Hz – 1 MHz and sampling frequency is reduced to address the lower part of the frequency range.

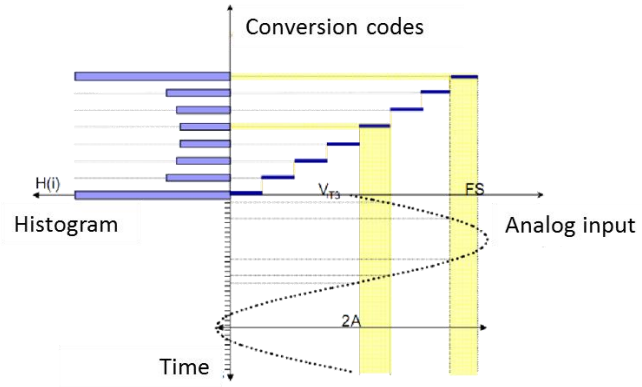

Figure 3. 3-bit histogram-based amplitude determination

This combined method proves robust to noise and allows addressing high frequencies while reducing consumption and design constraints. Synchronization or timing constraints are removed by this approach.

E. Data collection strategy

Usually, serial EIT systems use multiplexers to address different electrodes. This leads to high parasitic capacitances.

In this work, a commutation matrix built with reed relays allows to shift injection and measurement buses between electrodes: stray capacitances are minimized in this way. Commutation is driven by binary circular registers in the command module that are being transmitted to shift registers, driving the relays. To change injection and/or measurement configurations, the registers are merely shifted back and forth.

The design of the commutation matrix along with its command software lets freedom of choice for the data collection strategy. Offering choice of measurement patterns enable to maximize the sensitivity of measurements in correlation with the region of interest of the medium under study [12].

F. Performance assessment

Each elementary function of the system has been tested individually to assess if its performance matches the expectations. Signal generation has been examined for its steady output, bandwidth and low output impedance. Current-voltage conversion has been tried for its accuracy. Connection between analog and digital values has been reviewed.

TABLE 1. EXAMPLE TEST CELLS USED TO ASSESS PERFORMANCE

	R (Ω)	C (µF)
Test cells	10	
	1M	
	200	470e-3

Voltage controlled IS experiments are then performed on electronic test cells (Table 1). Using the Harvard Apparatus electrodes designed for rodent vagus nerve stimulation, *in vitro* and i*n vivo* measurements are also conducted, either with the electrodes dived in a saline bath, or with the electrodes acutely implanted around the left cervical vagus nerve of anesthetized rodents. These electrodes feature a 500µm inner diameter and two nerve-enwrapping contacts. Instrument behavior is verified on an electrical test cell featuring components that have been identified to depict the observed spectrum so as to determining the source of variation observed in impedance spectra.

Eventually, current controlled MfEIT is performed on a saline phantom of 4cm diameter featuring 14 equally-spaced copper electrodes. Measurements are carried out using a four-electrode method with an injected current of 100µApp at 98kHz or 5kHz. Inhomogeneities are created by the presence of either a 1cm diameter metallic cylinder or a 5mm diameter hollow insulating cylinder, i.e. $1/4$ or $1/8$ of phantom diameter.

G. Data collection and processing

For EIT, the EIDORS library [13] is used to perform direct and inverse problem calculations needed to reconstruct the conductivity distribution inside the medium under study. Inversion is conducted using a standard Tykhonov regularization with an empirical choice of hyperparameter [14].

III. RESULTS

A. Impedance spectra

Applying $10mV_{pp}$, the system features a bandwidth of 1kHz for impedances ranging from 100Ω up to 10MΩ, and a bandwidth of 1MHz for impedances ranging from 10Ω up to 100kΩ. Impedance spectra upon test cells have demonstrated that impedance norm is consistent by 3 dB and phase by 5° in the frequency range 0.1 Hz up to 1 MHz.

In vitro and *in vivo* two-electrode impedance spectra (Fig. 4) exhibit a behavior of a series circuit featuring a resistor and a capacitor. Measurements were only conducted until $100kHz$ due to noise issues. Impedance norm at 1kHz values 15kΩ *in vitro* and 12kΩ *in vivo*. Between *in vitro* and *in vivo* situations, similar impedance norms are observed, but a shift in the cutoff frequency occurs towards the lower part of the spectrum.

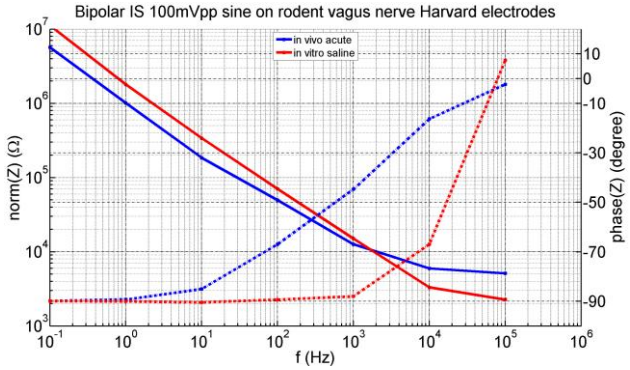

Figure 4. In vitro and in vivo impedance spectra; plain: impedance norm; dotted: impedance phase

B. Reconstructions from EIT

In vitro 3D temporal difference reconstructions of two positions of the metallic inclusion are conducted with the EIT system (cross section are shown in Fig. 5). Reconstructions are performed against acquisitions made for a homogeneous background.

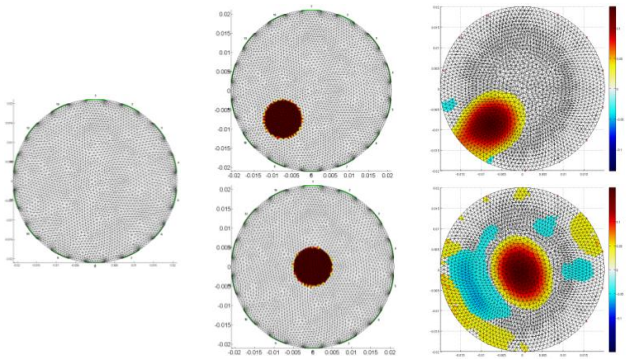

Figure 5. Cross-sections of 3D difference temporal reconstructions of one inclusion in conductive medium; right: inversion mesh; center: expected conductivity distributions; right: reconstructions

Data collected from the EIT system sounds consistent with the distribution of conductivity. Each measurement in the data collection protocol is conducted 10 times to assess the variation coefficient of the measurements: the estimated error shows a maximum value of 5% (maximum standard deviation of 11µV) with a mean value of 2%, which sounds adequate to proceed to reconstructions. In the reconstruction process, an equivalent homogeneous conductivity is estimated. Its value 1.60 S/m meets the concentration of the saline solution used for the experiments.

Frequency difference reconstructions have also been led to assess to multi-frequency capabilities of the proposed EIT system (Fig. 6). The inclusion is a 5mm diameter hollow insulating cylinder. Reconstruction are performed against a data set acquired at 5kHz versus another acquired at 98kHz. Data acquired in this operating framework also sounds to be consistent with the internal conductivity distribution.

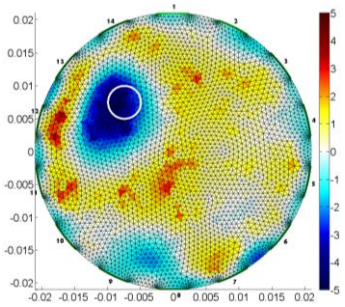

Figure 6. 2D frequency difference reconstructions of one hollow insulating inclusion, true position highlighted in white

IV. Discussion

In this work, a modular architecture of a combined IS and MfEIT system is presented. It offers ways to efficiently setup an experimental device for both EIT and IS. Under-sampling and commutation matrix concepts bring innovative solutions to match the demanding requirements for *in vivo* and *in vitro* electrical measurements. Under-sampling allows extending the frequency range while the relay commutation matrix features a low noise environment compared to multiplexers. Only amplitude measurements are kept for the EIT operation mode. Sign information is incorporated as a prior information in pre-processing.

Combining IS and EIT capabilities in a single system is difficult for low frequency electrical measurements. Limitation of such an approach stems from the low frame rate reached using this architecture: only low time constant phenomena can be monitored. A complete data collection for EIT is currently acquired in 45s.

System implementation has been validated following a system approach: elementary functions have been checked before assembly and overall performance assessment. Impedance spectra have been drawn from measurements upon known electrical test cells to calibrate the measurement system.

In vitro and *in vivo* experiments have been conducted under IS in order to evaluate the system answer in both environments. The measurement methodology used in this work ensures a proper interpretation of the impedance spectra and their variation.

In vitro tests have been performed in EIT and collected data seems consistent with the possibility of reconstructing images of internal conductivity distributions. 3D temporal difference imaging and 2D frequency difference imaging have been proposed to assess the capabilities of the system both in a single frequency mode and in a multi-frequency mode.

This work provides an experimental device that can be used to measure impedance spectrum and collect data for EIT reconstruction. It paves the way for future EIT tests that will include more complicated conductivity distributions, and *in vivo* experiments. Further investigation has to be done in the reconstruction process to better take into account the data and priors that can be included to constrain inversion algorithms.

The system proposed could benefit from an enhanced calibration procedure to correct for noise effects and components drifts that were observed during *in vivo* acquisitions. Eventually, the architecture and concepts developed in this work may be reused to broaden the bandwidth and adapted to increase frame rate.

References

[1] J. K. Seo and E. J. Woo, "Electrical Impedance Tomography," in *Nonlinear Inverse Problems in Imaging*, John Wiley & Sons, Ltd, 2013, pp. 195–249.

[2] D. Holder and Institute of Physics (Great Britain), *Electrical impedance tomography: methods, history, and applications*. Bristol; Philadelphia: Institute of Physics Pub., 2005.

[3] M. E. Orazem and B. Tribollet, *Electrochemical Impedance Spectroscopy*. Wiley, 2008.

[4] S. Grimnes and Ø. G. Martinsen, *Bioimpedance and Bioelectricity Basics*. Academic Press, 2008.

[5] A. McEwan, G. Cusick, and D. S. Holder, "A review of errors in multi-frequency EIT instrumentation," *Physiol. Meas.*, vol. 28, no. 7, pp. S197–215, Jul. 2007.

[6] "Raspberry Pi." [Online]. Available: http://www.raspberrypi.org/.

[7] "C library for Broadcom BCM 2835 as used in Raspberry Pi." [Online]. Available: http://www.airspayce.com/mikem/bcm2835/.

[8] "AD9837: LOW POWER, 8.5 mW, 2.3 V TO 5.5 V, PROGRAMMABLE WAVEFORM GENERATOR, Data Sheet Rev A, 12/2012."

[9] "LMV651 12 MHz, Low Voltage, Low Power Amplifier, Datasheet Rev J Mar 2013."

[10] "OPA380 High Speed Precision Transimpedance Amplifier, Datasheet Rev. G Sep 2007."

[11] "Low-Noise Voltage Preamplifier SR560 — DC to 1 MHz voltage preamplifier, Datasheet Rev. c."

[12] P. O. Gaggero, "Miniaturization and Distinguishability Limits of Electrical Impedance Tomography for Biomedical Application," 2011.

[13] A. Adler and W. R. B. Lionheart, "Uses and abuses of EIDORS: an extensible software base for EIT," *Physiol. Meas.*, vol. 27, no. 5, p. S25, May 2006.

[14] W. R. B. Lionheart, "EIT reconstruction algorithms: pitfalls, challenges and recent developments," *Physiol. Meas.*, vol. 25, no. 1, p. 125, Feb. 2004.